

Article

A New Technique for Reducing Size of a WPT System Using Two-Loop Strongly-Resonant Inductors

Matjaz Rozman , Michael Fernando, Bamidele Adebisi * , Khaled M. Rabie, Tim Collins ,
Rupak Kharel  and Augustine Ikpehai

School of Engineering, Manchester Metropolitan University, Manchester M1 5GD, UK;
rozmanmatjaz739@gmail.com (M.R.); m.fernando@mmu.ac.uk (M.F.); k.rabie@mmu.ac.uk (K.M.R.);
t.collins@mmu.ac.uk (T.C.); r.kharel@mmu.ac.uk (R.K.); augustine.ikpehai@stu.mmu.ac.uk (A.I.)

* Correspondence: b.adebisi@mmu.ac.uk; Tel.: +44-161-247-1647

Received: 13 September 2017; Accepted: 6 October 2017; Published: 16 October 2017

Abstract: Mid-range resonant coupling-based high efficient wireless power transfer (WPT) techniques have gained substantial research interest due to the number of potential applications in many industries. This paper presents a novel design of a resonant two-loop WPT technique including the design, fabrication and preliminary results of this proposal. This new design employs a compensation inductor which is combined with the transmitter and receiver loops in order to significantly scale down the size of the transmitter and receiver coils. This can improve the portability of the WPT transmitters in practical systems. Moreover, the benefits of the system enhancement are not only limited to the lessened magnitude of the T_X & R_X , simultaneously both the weight and the bill of materials are also minimised. The proposed system also demonstrates compatibility with the conventional electronic components such as capacitors hence the development of the T_X & R_X is simplified. The proposed system performance has been validated using the similarities between the experimental and simulation results. The power efficiency of the prototype circuit is found to be 93%, which is close to the efficiency reached by the conventional design. However, the weight of the transmitter and receiver inductors is now reduced by 78%, while the length of these inductors is reduced by 80%.

Keywords: wireless power transfer (WPT); efficiency; strongly-coupled magnetic resonance (SCMR)

1. Introduction

Induction-based wireless power transfer (WPT) technology is a thriving solution for variety of battery powered and battery-less apparatus in multiple application domains [1,2]. Research paradigm of WPT can be further elaborated using two fundamental concepts, namely, near field and far field. These terms indicate the interaction between the wireless receiver and the electromagnetic field. Furthermore, non-radiative near field indicates the induction at close proximity while far field indicates radiation at longer distances. Likewise, WPT possesses the ability to charge electrical devices, eliminating the use of conventional cable connections between the consumer and the grid. Besides its convenience, WPT technology also offers improvement in health and safety features in both domestic and commercial environments [3]. Although WPT can be acquired using radio-frequency (RF), microwaves or laser beams (LB) [4,5] the main focus of this paper will solely be on power transmission via inductive coupling (IC).

Recently, a great number of attempts have been made towards the deployment of inductive WPT technology, to be used as a main energy source for battery-less devices. Regardless of the fact that prevailing technologies have been designed with a specific application in mind, WPT has been widely adapted in applications ranging from smart phones, consumer electronics, vehicle charging to medical

applications which include portable medical devices, smart animal tracking systems, surgical tools and implantable medical devices [6–8]. The majority of portable devices use built-in batteries for power source, therefore a WPT system seems a convenient way to provide power to batteries in the electrical devices such as smart phones, electric vehicles, toothbrushes, etc. [9,10]. The power is delivered wirelessly over the air gap, however most of the chargers use plastic or metal cover. The transmitter reaches the charging device via an electromagnetic field as presented in Figure 1 [11–13].

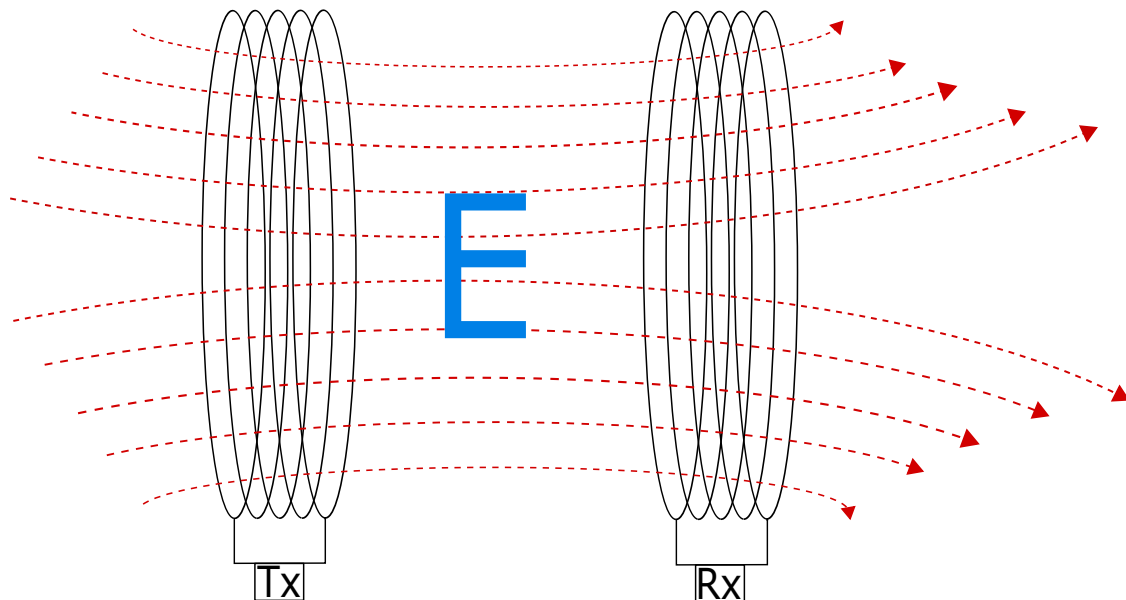


Figure 1. Electromagnetic field between the transmitter and receiver loops, which occurs due to changing polarity of the current flow.

The need for an industry standard for WPT emerged with the increasing popularity of WPT charging devices. As an answer to that a wireless power consortium has introduced the Qi standard [14–16]. The standard was adopted for both low and medium power transmission, and it allows to charge the device with the power of up to 5W. Increasing both the power transmission efficiency and the distance between the coils plays a vital role in the development of WPT systems [17,18]. The efficiency of the system is highly dependent on distance and the alignment between the transmitting and receiving coils [19,20]. Over the past few years, many techniques have been applied to optimise the transfer efficiency over low coupling factor [21]. Compensation topology and circuit analysis play the most fundamental role in the design of resonant WPT systems [22]. To improve the system distance, high quality factor (Q) of the coil is a crucial element [23], however this requires the coil to have much higher inductance over capacitance, and therefore increased value of the Q makes the coil bulky [24].

Also, it is important to note that the Qi standard is not suitable for higher power applications such as electrical vehicle charging [25–27]. Qi technique uses loosely-coupled loops, however, with the use of strongly-coupled magnetic resonance (SCMR) technique researchers were able to achieve much higher transfer efficiency at smaller coupling factors [28,29]. Critically coupled resonators can be used in order to gain highest efficiency of the SCMR system [30,31]. Quality factor of the coil plays a crucial role in achieving high efficiency at low coupling factor, therefore the inductance of the coil must be relatively high in relation to the capacitance [32,33].

The size of the WPT system has gained widespread popularity among researchers, since the market interest of being applicable to real time problems increased. Researchers have made numerous attempts towards the reduction of the coil size [34,35]. In [32], the use of embedded loops in a SCMR system has been suggested by the authors. Conformal SCMR (CSCMR) system indicates a significant

reduction of the size of four-loop systems. Authors in [36] have also suggested using metamaterial arrays and a three coil system to further reduce the size of the receiver. Series-series connected resonant capacitors with a double current rectifier, has been proposed in [37]. Furthermore, according to the authors this method simultaneously reduces the current in the secondary coil while the physical parameters of the coil are reduced. A significant reduction of 38% of a total coil weight has been gained in [38], where the authors proposed a selective harmonic approach of the transfer frequency.

In this paper, we explore the possibility of introducing a new set of inductors to the existing transmitter and receiver structure in order to further reduce their size. While the new technique reduces both the size and the weight of the coils with minimum compromise in efficiency, it further reduces the amount of the material used for the circuit simultaneously leading to minimised production cost. This will make the resonant WPT system more desirable in handheld applications. The contributions of this paper are as follows. Initially, the analytical model of the newly proposed system with additional inductors, indicates that the system reaches its maximum efficiency at a lower coupling coefficient. In addition, the relationship between the size of the new inductors and the coupling factor needed to reach maximum efficiency is studied. Also the effect of the resistance of additional coils on the system efficiency is investigated. The second contribution of this work resides in conducting experiments in order to validate the analytical results. Furthermore, a novel concept of designing a two-loop resonant WPT circuit is introduced, where instead of using resonant inductors with a high resonant factor, a set of small inductors is placed in parallel with an inductor of a low quality factor. The technique allows the newly formed WPT circuit to reach its maximum efficiency at similar or even smaller coupling factor as the circuit with the coils of high quality. Results demonstrate that the proposed system is able to achieve similar efficiencies as the system with larger coils at similar distances, interestingly, with further reduction in size and weight. This further indicates that the high quality of the system can be achieved without higher inductive coils and specific, lower capacitors value.

The rest of the paper is structured as follows. Section 2 describes the proposed model and presents the mathematical analysis providing an insight into the subject using multiple theoretical equations, while the system specifications and numerical results are presented in Section 3. In Section 4, the experimental parameters and the system configuration are described in details. A comparison between the calculated and the measured coupling factors needed to reach the maximum efficiency is made in Section 5. Finally, the conclusions are drawn in Section 6.

2. Theoretical Analysis of Strongly-Coupled WPT Systems

In highly resonant WPT systems the resonators must have a high resonance factor in order to transfer energy efficiently across the gap between the transmitter and receiver coils. When two resonators are placed close to each other they form an inductive link which allows them to transfer energy via mutual inductance (M), as shown in Figure 2a. The electromagnetic field (H) between the two loops can be derived from Ampere's law and Faraday's law of electromagnetic induction [39] as:

$$H_y = \int \Delta H_y = \frac{I_x r_y^2}{2 (r_y^2 + d^2)^{\frac{3}{2}}} \quad (1)$$

where I_x represents the current in x th loop, r_y is the radius of y th loop, while d represents the distance between the two loops.

As shown in Figure 2b, the proposed system introduces two inductors in parallel with an existing inductor. The newly added inductors are minimised in size and are positioned in the circuit in a way to have no effect on the mutual inductance link between the transmitter and the receiver coils.

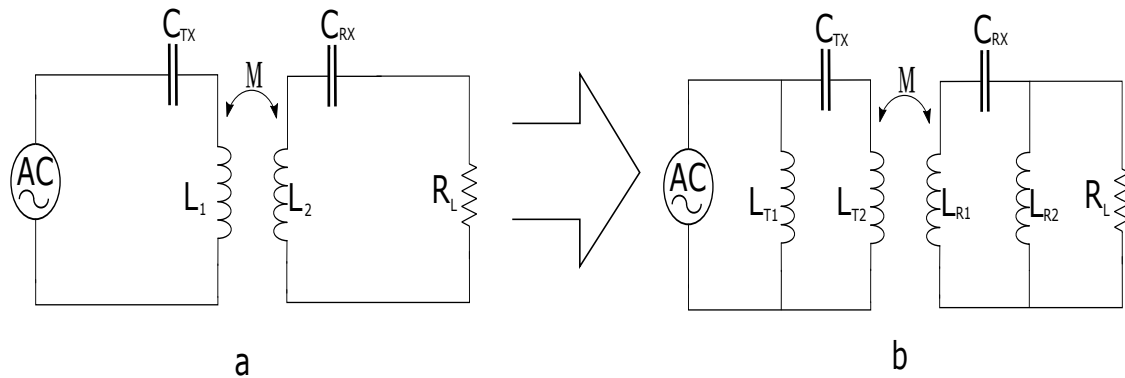


Figure 2. (a) A comparison between the conventional WPT system with a single set of coils ; and (b) the proposed technique with an additional coil.

The WPT circuit model of the proposed topology is presented in Figure 3. In addition to the existing LC resonant loop, this method introduces two additional inductors, one on each side of the WPT system. At the transmitter side, the new inductor L_{T2} is placed in parallel to the pre-existing LC oscillator and forms a new LCL circuit design. Similar to the transmitter side, the receiver has a new inductor attached in parallel with preexisting LC circuit and forms a new LCL oscillating circuit on the receiver side. The two newly formed oscillators determine the oscillating frequency of the WPT circuit, at which the transmitted power will be maximised. In addition to the two inductors L_{T2} and L_{R2} , the circuit contains a frequency generator (AC) used as a power source and its input is a sine-wave voltage, while RG represents the internal resistance of the frequency generator. C_{TX} and C_{RX} are the transmitter and receiver capacitors which together with L_{T1} , L_{R1} , L_{T2} and L_{R2} form the LC oscillator. It is important to note that the real inductor already has some self capacitance reduce value and therefore the loop already has its own oscillating frequency. However, in order to reduce magnitude of the current and increase the magnitude of the voltage, compensation capacitors must be added [18]. R_{LT1} , R_{LT2} , R_{LR1} and R_{LR2} represent the internal resistance of the used inductors.

To analyse the circuit, all branches currents and voltages should be determined. At the transmitter side the I_{IN} represents the input current. The current I_{IN} is divided into two currents, I_2 and I_3 based on Amperes law ($I_{IN} = I_2 + I_3$). Voltage V_A represents the voltage on the T-node at the transmitter. At the receiver side, I_4 represents the induced current through mutual inductance (M) from the transmitters coil L_{T1} to the receiver coil L_{R1} , the current is further divided into two currents I_5 and I_6 ($I_4 = I_5 + I_6$) while V_B represents voltage at the T-node at the receiver side. R_L represents the resistance of the load, while Z_{T1} , Z_{T2} , Z_{R1} and Z_{R2} are the impedances of the inductors. The impedance is calculated as $Z_X = R_X + j\omega L_X$, where R_X represents an internal resistance of each inductor, and L_X represents inductance.

The energy normally oscillates between the coil and the capacitor. The angular frequency at which the energy oscillates can be mathematically calculated as $\omega_0 = \frac{1}{\sqrt{LC}}$. However, in the proposed design the additional coil is introduced, therefore the energy oscillates between the capacitor and the two inductive coils, and can be expressed as:

$$\omega_0 = \frac{1}{\sqrt{C(L_X + L_Y)}} \quad (2)$$

A desired oscillating frequency of the system can be adjusted with the size of inductor and capacitor, however in order to achieve higher distances a high quality factor is required. The quality factor can be calculated as:

$$Q = \sqrt{\frac{L_X}{C_X} \frac{1}{R_X}} \quad (3)$$

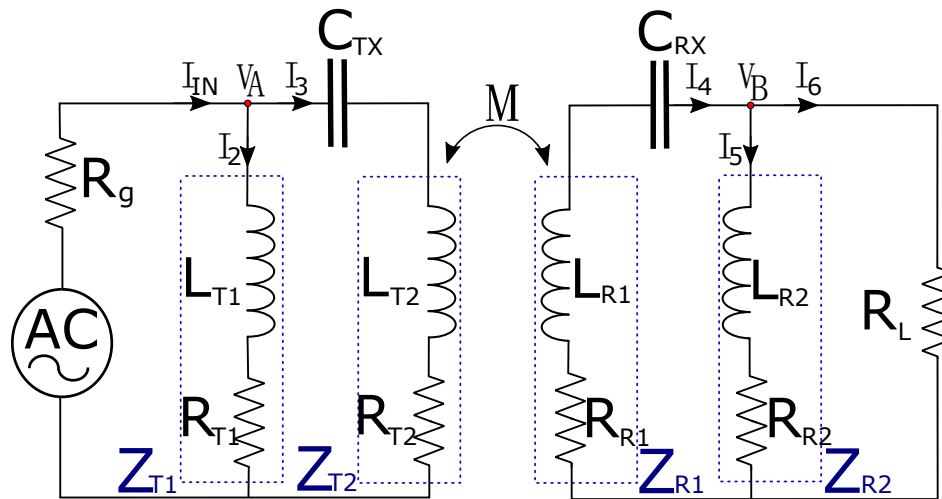


Figure 3. The circuit diagram of the proposed two-loop resonant WPT system with additional inductor. I_{IN} , I_2 , I_3 , I_4 , I_5 and I_6 represent the currents in each branch, while the Z_{T1} , Z_{T2} , Z_R and Z_{R2} represent impedance of the inductors.

High quality factor of the resonators is crucial for a high-resonant WPT system to achieve high efficiency. Resonators are usually made to have a relatively narrow frequency band which reduces their chance to interact with other objects. However, in order to achieve a high quality factor high inductance is required, that increases the size of the transmitter and receiver loops. In order to reduce the size of the transmitter and receiver loops, a new concept of design is proposed. With the LCL design herein described, in which the inductors are placed in a way that only T_X and R_X inductors interact with each other, similar results can be obtained. In order to analyse the circuit of the proposed system, the following set of equations can be derived from the proposed circuit in Figure 3, and the currents in the circuit can be mathematically described as:

$$i_2 = \frac{V_A}{(R_{T1} + j\omega L_{T1})} \quad (4)$$

$$i_3 = \frac{V_B - (i_4 j\omega M)}{(R_{T2} + j\omega L_{T2} + \frac{1}{j\omega C_{TX}})} \quad (5)$$

$$i_4 = \frac{-(V_B + (i_3 j\omega M))}{(R_{R1} + j\omega L_{R1} + \frac{1}{j\omega C_{RX}})} \quad (6)$$

$$i_5 = \frac{V_B}{(R_{R2} + j\omega L_{R2})} \quad (7)$$

and the voltage V_A can be written as:

$$V_A = V_{IN} - ((i_2 + i_3)R_G) \quad (8)$$

while the voltage V_B is:

$$V_B = (I_4 - I_5)R_L \quad (9)$$

In order to reduce the complexity of the calculation, the following part of the equation has been simplified:

$$\begin{cases} Z_1 = R_{LT2} + j\omega L_{LT2} \\ Z_2 = R_{LT1} + j\omega L_{LT1} \\ Z_3 = R_{LR1} + j\omega L_{LR1} \\ Z_4 = R_{LR2} + j\omega L_{LR2} \\ C_{TX} = \frac{1}{j\omega C_{TX}} \\ C_{RX} = \frac{1}{j\omega C_{RX}} \end{cases} \quad (10)$$

Therefore, from these equations the input impedance Z_{IN} can be calculated as:

$$Z_{IN} = \frac{(aZ_{T1} + bZ_{T2} + cZ_{R2} + dZ_{T1} + eR_L R_G Z_{R1} + (C_{RX} C_{TX} - M^2) R_L R_G)}{(fZ_{T2} + gZ_{T1} + hR_L Z_{R1} + (C_{RX} C_{TX} - M^2) R_L)} \quad (11)$$

where

$$\begin{cases} a = Z_{R2}(Z_{R1} + R_L + C_{RX}) + R_L Z_{R1} + C_{RX} R_L \\ b = (R_G Z_{R1} + (R_L + C_{RX}) R_G) Z_{R2} + R_L R_G Z_{R1} + C_{RX} R_L R_G \\ c = ((R_G + C_{TX}) Z_{R1} + (R_L + C_{RX}) R_G + C_{TX} R_L - M^2 + C_{RX} C_{TX}) Z_{R2} \\ d = (R_L R_G + C_{TX} R_L) Z_{R1} + C_{RX} R_L R_G + (C_{RX} C_{TX} - M^2) R_L \\ e = (C_{TX} R_G Z_{R1} + (C_{TX} R_L - M^2 + C_{RX} C_{TX}) R_G) Z_{R2} + C_{TX} \\ f = (Z_{R1} + R_L + C_{RX}) Z_{R2} + R_L Z_{R1} + C_{RX} R_L \\ g = Z_{T1}(Z_{R1} + R_L) + C_{RX} Z_{R2} + R_L Z_{R1} + C_{RX} R_L \\ h = (C_{TX} Z_{R1} + C_{TX} R_L - M^2 + C_{RX} C_{TX}) Z_{R2} + C_{TX} \end{cases} \quad (12)$$

The efficiency of the system η , can be calculated as:

$$\eta = \frac{P_{OUT}}{P_{IN}} = \frac{i_{OUT}^2 Z_{IN}}{i_{IN}^2 Z_{EQ}} \quad (13)$$

Therefore, the efficiency of the proposed circuit could be expressed as follows:

$$\eta = \frac{-MR_L Z_{R2} Z_{T1}}{kZ_{T1} + lZ_{T2} + mZ_{R2} + nZ_{T1} + oZ_{R2} + C_{TX} R_L R_G Z_{R1} + pR_L R_G} \quad (14)$$

where k, l, m, n, o and p are:

$$\begin{cases} k = (Z_{R1} + R_L + C_{RX}) Z_{R2} + R_L Z_{R1} + C_{RX} R_L \\ l = (R_G Z_{R1} + (R_L + C_{RX}) R_G) Z_{R2} + R_L R_G Z_{R1} + C_{RX} R_L R_G \\ m = (R_G + C_{TX}) Z_{R1} + (R_L + C_{RX}) R_G + C_{TX} R_L - M^2 + C_{RX} C_{TX} \\ n = (R_L R_G + C_{TX} R_L) Z_{R1} + C_{RX} R_L R_G + (C_{RX} C_{TX} - M^2) R_L \\ o = C_{TX} R_G Z_{R1} + (C_{TX} R_L - M^2 + C_{RX} C_{TX}) R_G \\ p = (C_{RX} C_{TX} - M^2) \end{cases} \quad (15)$$

G is gain for the circuit and can be expressed as:

$$G = MR_G Z_{T1} (Z_{T2} + C_{TX}) ((r) Z_{T1} + R_G V_B q Z_{R2} + R_L R_G V_B(q)) \quad (16)$$

where q and r can be described as:

$$\begin{cases} q = V_B(Z_{R1} + R_L + C_{RX})Z_{R2} + R_L V_B(Z_{R1} + C_{RX}) \\ r = Z_{T2}(sZ_{T1} + R_G V_B t) + (u + MR_L V_{IN})Z_{R2} + V_{BZ} \end{cases} \quad (17)$$

and the o , p , q and r are:

$$\begin{cases} s = (Z_{R1} + R_L + C_{RX})Z_{R2} + R_L R_G V_B (Z_{R1} + C_{RX}) \\ t = V_B (R_G (Z_{R1} + R_L + C_{RX}) + C_{TX} (Z_{R1} + C_{RX})) + C_{TX} R_L - M^2 \\ u = R_L (C_{TX} (Z_{R1} + C_{RX}) - M^2) + R_L R_G (Z_{R1} + C_{RX}) \\ z = C_{TX} (Z_{R1} + C_{RX}) + C_{TX} R_L - M^2 \end{cases} \quad (18)$$

3. Numerical Analysis

The transmission efficiency and the distance at which the system achieves maximum efficiency strongly depends on the geometrical design of the loops [40], and can be calculated as:

$$M_{XY} = M_{YX} = \frac{\Psi_{XY}}{I_X} = \frac{\mu_0 H_Y A_Y}{I_X} = \frac{\mu_0 r_Y^2 r_X^2 \pi}{2\sqrt{(r_X^2 + d^2)^3}} \quad (19)$$

In order to compare the results between two designs, all four loops which oscillate at the same frequency have been designed to have the same inner diameter. The inner diameter of the transmitter and receiver loops were set to be at 72 mm and the frequency at which they oscillate was set at 9.23 MHz. However, as presented in (19), an inner diameter of the loops can be chosen as desired, without affecting the results. If the inner diameter is reduced, the maximum efficiency will be at the same coupling factor between the two loops as for the larger system. The additional loops (L_{T1} , L_{R2}) have a diameter of 2 mm, however, they do not affect the mutual inductance between the transmitter L_{T2} , and receiver L_{R1} coils.

3.1. High Q Coil System Specifications

According to (3), the requirements that determine the Q of the coil are low resistance of the coil and high ratio between the inductance and capacitance. However, the combination of the inductor and capacitor plays a vital role in determining the oscillating frequency. Therefore, to calculate the parameters of the high Q loop, Equation (2) has to be considered. Calculated values of the elements used in high Q circuit are presented in Table 1. The inductance of the transmitter loop (L_1) is set at 186.6 μ H while the required capacitance is $C_1 = 1.6$ pF. For the receiver loop, the inductance L_2 is set at 229.6 μ H while the capacitance of the receiver is $C_2 = 1.3$ pF. The internal resistance of the coils is 0.15 Ω whereas the resistance of the source and load is equal to 50 Ω .

The simulation results of the above circuit are presented in Figure 4. It is shown from the figure that when the coupling factor between the transmitter and the receiver is 0.1, the circuit is over-coupled. The maximum efficiency appears at the frequency of 8.79 and 9.71 MHz. The maximum efficiency of the circuit appears when the coupling factor between the transmitter and receiver is 0.004 and after optimum coupling factor is reached the efficiency starts to decline. When the coupling factor falls to 0.001, the maximum efficiency declines to 43%.

Table 1. Calculated elements of two-loop strongly coupled WPT system with high Q of coils, used to build a practical system.

Capacitance	Inductance	Resistance	Resistance
$C_1 = 1.6 \text{ pF}$	$L_1 = 186.6 \text{ } \mu\text{H}$	$R_{L1} = 0.15 \text{ } \Omega$	$R_S = 50 \text{ } \Omega$
$C_2 = 1.3 \text{ pF}$	$L_2 = 229.6 \text{ } \mu\text{H}$	$R_{L1} = 0.15 \text{ } \Omega$	$R_L = 50 \text{ } \Omega$

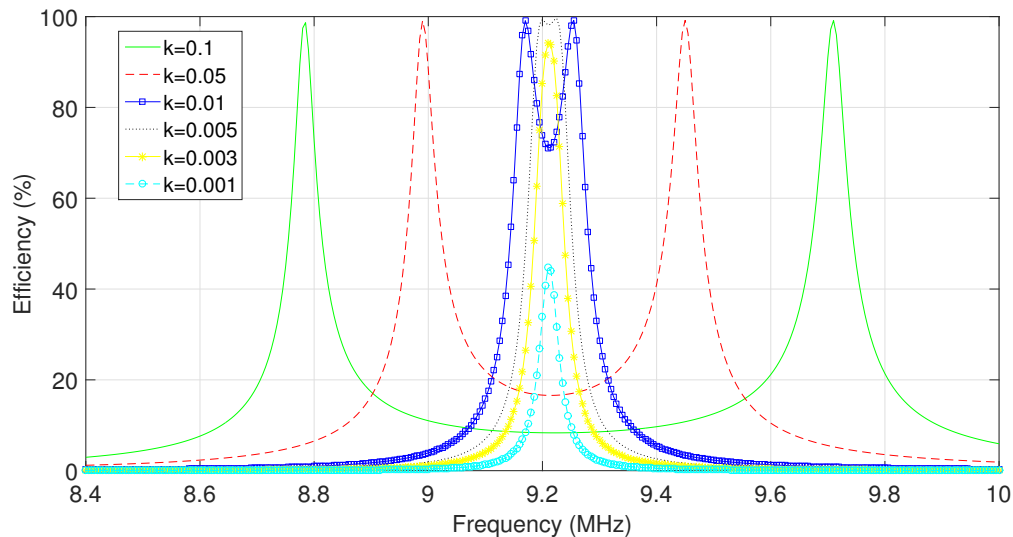


Figure 4. Calculated efficiency of the system with high Q of the transmitter and receiver coils, built based on the value of the elements from Table 1.

3.2. Low Q Coil System Specifications without Additional Inductor

In contrast to the high Q system, the loops in this system do not require a large capacitance and inductance ratio, as presented in Table 2. In order to make the system more cost-effective, standard widely available 15 pF and 18 pF capacitors were used in this experiment. The capacitance value for the system with Low Q coil is much higher than that of the capacitors used for high Q design, however the market price per unit is similar. Therefore, to make the loops oscillate at the same frequency as the system with high Q inductors, the transmitter loop must have inductance of 16.37 μH and 19.65 μH , respectively. The resistance of the inductors is the same as the resistance of the loops with high Q, 0.15 Ω .

In Figure 5 the calculated performance of the system is presented. As shown in this figure, the system reaches maximum efficiency when the coupling factor between the transmitter and receiver is equal to 0.05, which is far higher than the coupling factor required to reach maximum efficiency with high Q of the coil at 0.004. The system with low Q factor reaches efficiency of 15% at the coupling factor of 0.003, which is equivalent to 81% reduction compared to the previous system.

Table 2. Calculated base model of two-loop loosely coupled WPT system. The specification will be later used to build a practical model.

Capacitance	Inductance	Resistance	Resistance
$C_1 = 18 \text{ pF}$	$L_1 = 16.37 \text{ } \mu\text{H}$	$R_{L1} = 0.15 \text{ } \Omega$	$R_S = 50 \text{ } \Omega$
$C_2 = 15 \text{ pF}$	$L_2 = 19.65 \text{ } \mu\text{H}$	$R_{L1} = 0.15 \text{ } \Omega$	$R_L = 50 \text{ } \Omega$

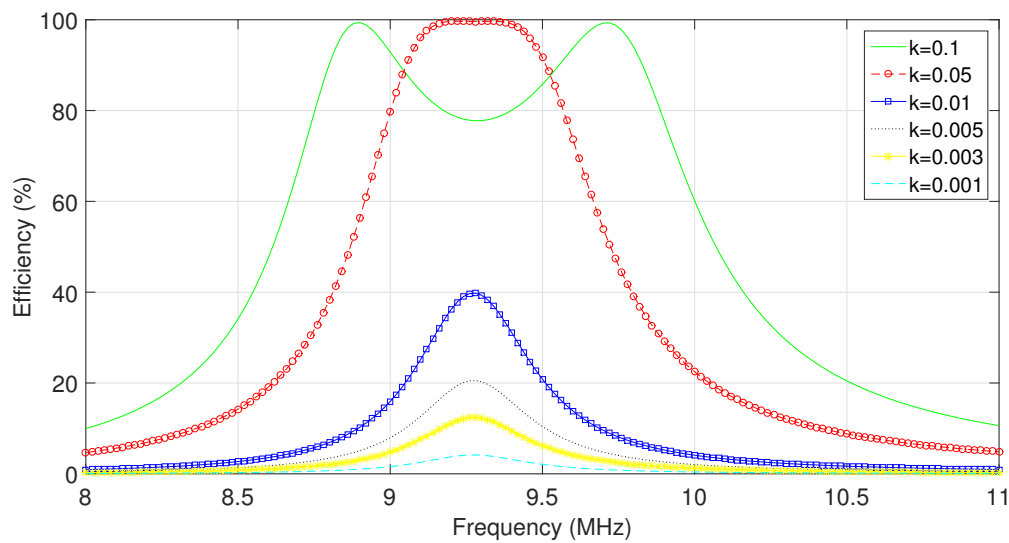


Figure 5. Efficiency of the system with low Q factor of the coil without additional inductor, calculated with advanced design system (ADS) software. A coupling factor at which maximum efficiency appears is much higher than that for the system with high Q.

As mentioned earlier, the quality of the coil affects the coupling factor needed for the system to reach maximum efficiency. In Figure 6 the difference between the two systems is presented. It is evident that the system with low Q value requires higher coupling factor to gain its maximum efficiency. However, the system designed with high Q value has its maximum efficiency at the coupling factor of 0.004 while the system with low Q coils obtains maximum efficiency when the quality factor is 0.05.

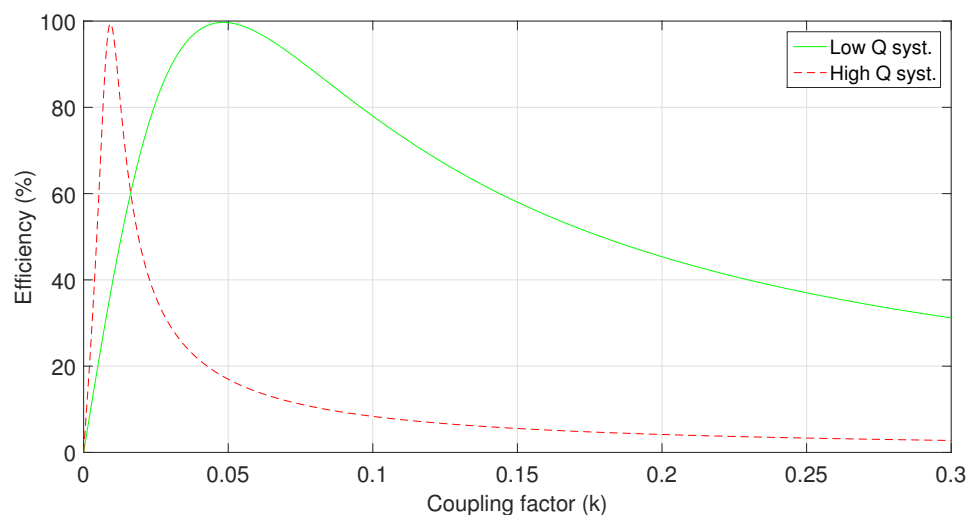


Figure 6. Comparison between the coupling factor needed for the maximum efficiency to appear for the system with low Q and high Q of the coils.

To enhance the performance of the system with low Q coils, two new inductors are introduced to the existing WPT system. The inductors L_{T1} and L_{R2} are connected in parallel with the transmitter and receiver loops, (L_{T2} , L_{R1}). In order to determine the size of the additional coils, the graphical presentation of the effect is presented in Figure 7. It is shown that the increase of the value of the additional inductors connected in parallel to the resonator coil increases the coupling factor needed to maximize the efficiency. If $L_{T1} = 2.105 \mu\text{H}$ and $L_{R2} = 2.359 \mu\text{H}$, the difference between the coil with

additional inductors and low Q coil is minimal. Conversely, if the additional inductors values are too small, as shown in the figure where the $L_{T1} = 0.02105 \mu\text{H}$ and $L_{R2} = 0.02359 \mu\text{H}$ are used, the maximum efficiency drops drastically.

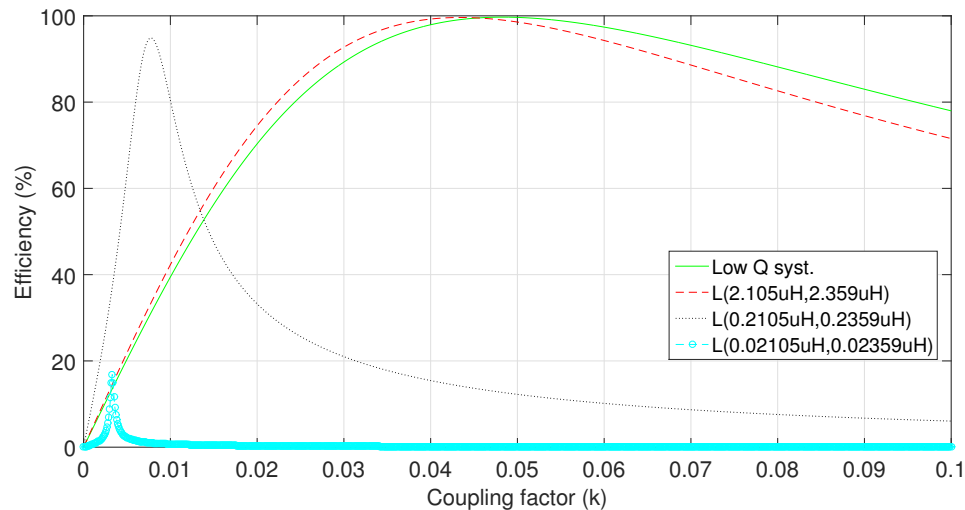


Figure 7. The effect of the different values of additional inductors on the coupling factor needed to reach maximum efficiency. The coupling factor needed to reach maximum efficiency drops with the decrease of the value of additional inductor.

The size of the additional inductors has to be chosen based on the numerical analysis. In this case, we chose to use $L_{T1} = 0.2105 \mu\text{H}$ and $L_{R2} = 0.2359 \mu\text{H}$ which offer a performance close to that of the system with high Q of the inductor, as shown in Figure 8. To maintain the oscillating frequency of the system at 9.23 MHz and to use the widely produced capacitors, a tradeoff in performance is required. Therefore, the designed system reaches the maximum efficiency at $k = 0.003$, while the system with high Q factor reaches its maximum at $k = 0.004$.

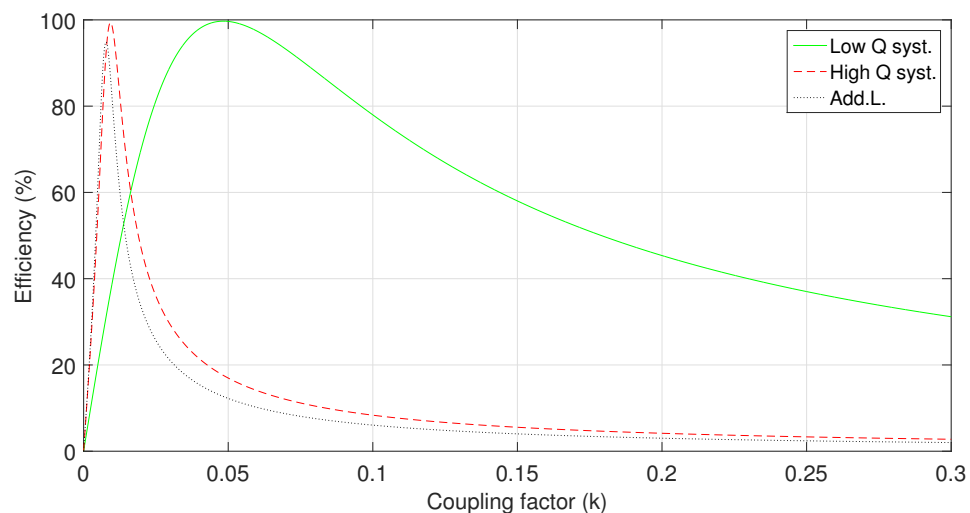


Figure 8. Comparison of the maximum distance between the T_X and R_X loops of the system with low Q design, with and without additional inductors and a system with high Q coil design.

The system specification of the elements is presented in Table 3. As it can be seen, the system is a combination of the low Q coils and the additional coils. The calculated performance of the system is

presented in Figure 9. As shown in the figure, the system reaches a maximum efficiency of 95% when the coupling factor between the transmitter and receiver is 0.003. This presents high improvement over the system with low Q coils which reaches maximum efficiency at $k = 0.05$. However, an efficiency drop is a major drawback which is a reasonable trade-off in order to reach larger distance without affecting the coils size and weight.

Table 3. Calculated values of the elements used in the proposed model with two loop loosely coupled WPT system with a low Q of the coils and two additional inductors.

Capacitance	Inductance	Resistance	Resistance
$C_{TX} = 18 \text{ pF}$	$L_{T2} = 16.37 \text{ } \mu\text{H}$	$R_{L2} = 0.15 \text{ } \Omega$	$R_L = 50 \text{ } \Omega$
$C_{RX} = 15 \text{ pF}$	$L_{T1} = 0.2105 \text{ } \mu\text{H}$	$R_{T1} = 0.15 \text{ } \Omega$	$R_L = 50 \text{ } \Omega$
	$L_{R1} = 19.65 \text{ } \mu\text{H}$	$R_{R1} = 0.15 \text{ } \Omega$	
	$L_{R2} = 0.2359 \text{ } \mu\text{H}$	$R_{R2} = 0.15 \text{ } \Omega$	

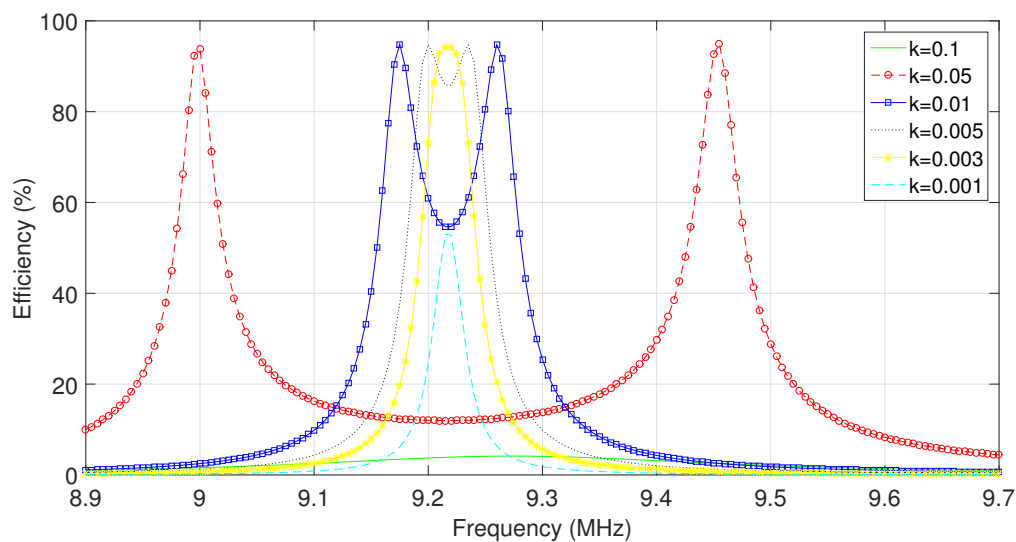


Figure 9. Calculated efficiency of the proposed system with low Q of the coils with two additional inductors. The coupling factor at which maximum efficiency is much smaller than that for the low Q design without additional coils.

3.3. Effect of the Additional Coil Resistance on the System Efficiency

The resistance of the added coils R_{LT2} and R_{LR2} has an important impact on the maximum efficiency thus has been analytically determined via mathematical calculations, which has been the base of the Figure 10. It can be seen that increasing the resistance of the added inductors has a negative effect on the transmission efficiency. When the resistance of the added coils increases from $0.1 \text{ } \Omega$ to $0.5 \text{ } \Omega$, the system efficiency drops by 10%. A further increase in the coils resistance to $1 \text{ } \Omega$ leads to a drop of efficiency by additional 10% to 70%. From the figure it can be concluded that the increase in resistance leads to a rapid decrease in the system efficiency. However, in the opposite direction, when the resistance decreases, the efficiency improves. As seen from the graph, when the resistance decreases from $0.1 \text{ } \Omega$ to $0.001 \text{ } \Omega$, the efficiency of WPT system increases by 1%, to 95%. Therefore, in order to reach high efficiency, maintaining a low resistance of added coils R_{LT2} and R_{LR2} is a crucial factor.

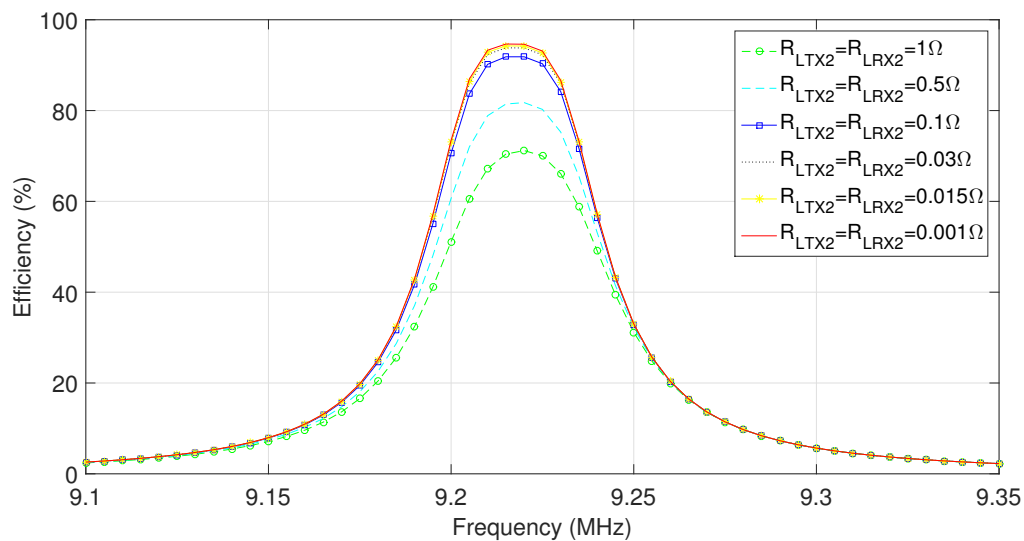


Figure 10. Effect of different resistance of added coils on the systems efficiency. The smaller the resistance, the higher the efficiency and vice-versa.

4. Experimental Setup

An experimental setup is presented in this section. In order to verify the calculated results, an appropriate system was built. A pair of loops were designed for this experiment as shown in Figure 11a. The first pair is the conventional T_X and R_X loops shown at the left side of the figure and the second pair is the modified T_X and R_X loops. A practical implementation of the measurement setup can be seen in Figure 11b.

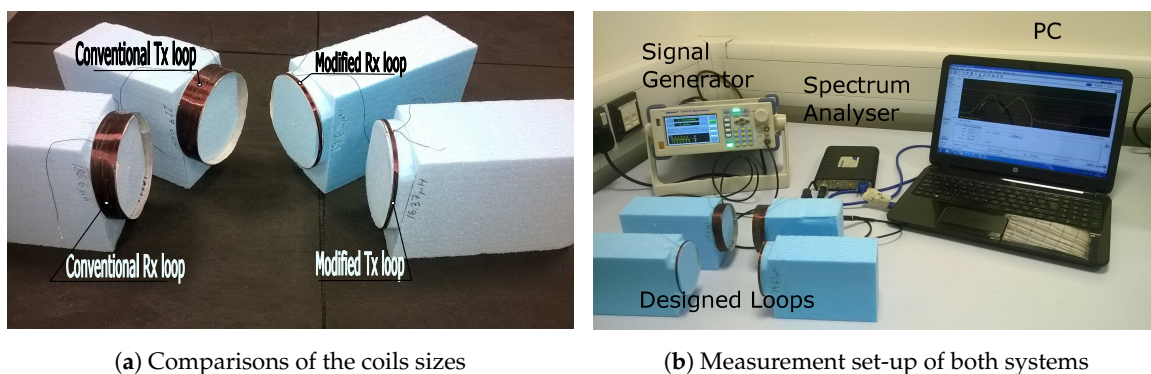


Figure 11. Practical implementation of the proposed model along with the required requirement.

4.1. System Design and Measurements

Both systems consist of single T_X and R_X loops, made of the same enameled copper wire. The conventional T_X loop is made of 41 turns while the conventional R_X loop contains 48 turns. In contrast, the modified T_X and R_X loops are made of only 8 and 9 turns, respectively. All loops have the same diameter of 72 mm. In addition to the T_X and R_X loops, the proposed system contains two additional inductors made with the same material. The additional inductors L_{T1} and L_{R1} are made of 2 and 3 turns respectively and both have inner diameters of 3 mm. In order to tune the loops to oscillate at the same frequency, ceramic capacitors were used.

A signal generator Digimess SG200 RF was used to provide circuit with various frequency signals, which were applied to the T_X loop. Measuring frequency response of the loops plays important

role in order to compare quality of the loops and their oscillating frequency. Its also shows good comparison between the calculated and designed loops performance. The response of the circuit was measured at the R_X loop, and it was carried out by a USB-based spectrum analyser, the Tektronix RSA306. The spectrum analyser was connected to a computer-based software where the results of the measurements were finally displayed.

4.2. System Maximum Efficiency

According to the calculation, for the modified system, an optimal efficiency appears when the coupling factor between the T_X and R_X loops is equal to 0.003. As Figure 12 shows a maximum efficiency of the modified system reaches 96% at a frequency of 9.25 MHz. The measurements confirm that the designed system follows the frequency pattern of the calculated system. The maximum efficiency is reached at a frequency of 9.23 MHz, however the reached maximum efficiency is slightly below the calculated value at 89%. The same system at the coupling factor $k = 0.01$ suffers the effect of frequency splitting and reaches a double peak at frequencies of 9.17 MHz and 9.26 MHz. The measured results once again confirm the calculated values, a measured double peak maximum efficiency is reached at frequencies of 9.155 and 9.265 MHz. Maximum efficiency is again slightly lower than the calculated values and measured at 85% and 87%, which are 10% and 8% lower than the calculated value.

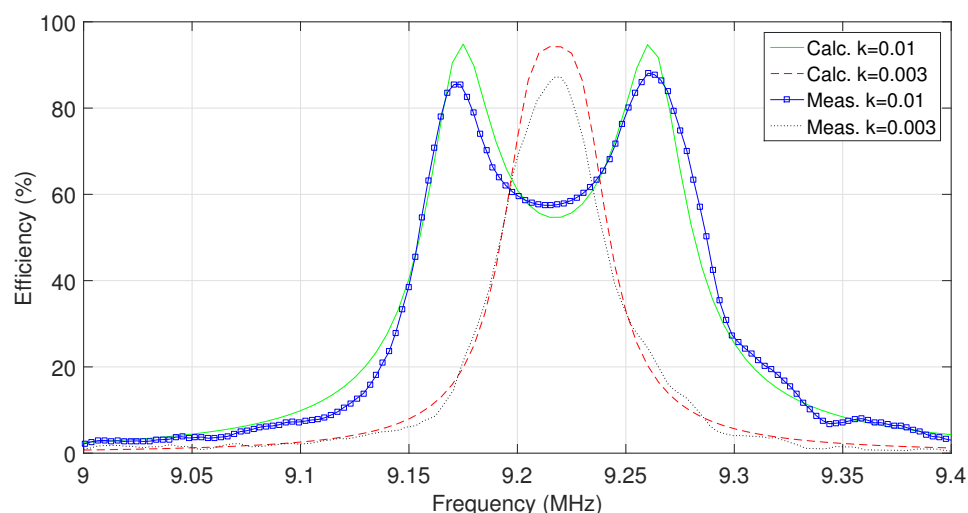


Figure 12. Comparison between the measured and calculated maximum efficiency and frequency pattern for the modified circuit with additional coils. The results show close similarity of calculated and measured results.

In contrast to the modified loops, the conventional system has slightly wider frequency spectrum. The main reason for this is that in order to use widely produced capacitors for the modified system, the quality factor of the combined coil must be slightly higher than the one from conventional systems in order for both systems to oscillate at the same frequency. That is also the reason for the efficiency drop at the frequency 9.23 MHz, since the system is already in decline at coupling factor of 0.003, as we can see in Figure 13. Also in Figure 13 it can be seen that the measured efficiency at frequency 9.23 MHz is 3% below the calculated value, for $k = 0.003$. It is evident that the measured efficiency for both coupling factors, $k = 0.003$ and the $k = 0.01$ resemble the calculated pattern. Double peaks at 9.15 MHz and 9.28 MHz as indicated in Figure 13, where $k = 0.01$ indicates a difference of 0.01 and 0.005 MHz compared to the calculated results.

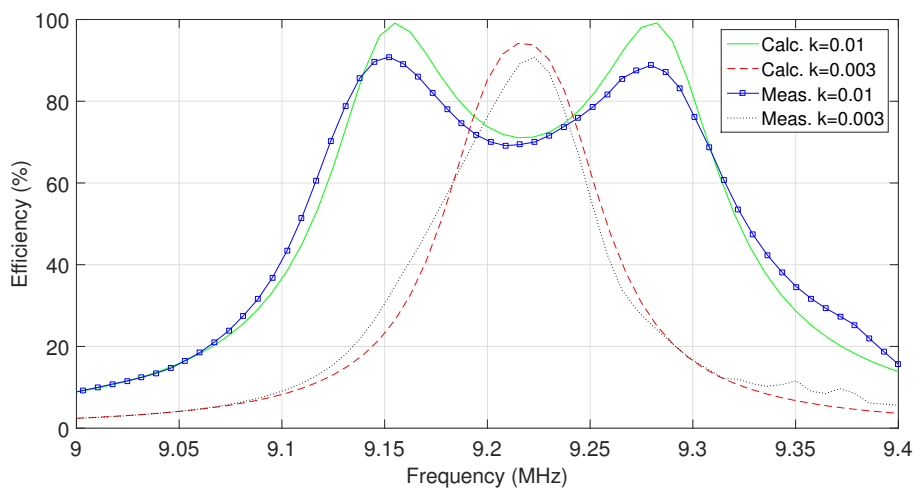


Figure 13. Comparison between the measured and calculated maximum efficiency and frequency pattern of the conventional system with a high Q of the coil. A designed system shows close similarities with the calculations.

5. Results

The maximum distance at which the system is able to deliver power with high efficiency is a crucial factor in any WPT system. Up until now a high quality factor of the transmitting and receiving coils was required to efficiently transmit the power on small coupling factor between the two coils. With the proposed method for the maximum distance of the transmission, the quality factor of the transmitting and receiving coils can be made smaller. As shown in Figure 13 the maximum transmission efficiency between the two coils with low quality factor occurs when the coupling factor between them is equal to 0.05. However, the same two coils can achieve larger maximum distance for the power transfer with the addition of two small inductors L_{T1} and L_{R2} in parallel with the existing inductors. The maximum power transmission between two coils in that case occurs when the coupling factor between the two coils is equal to 0.003, which significantly improves the maximum distance. In both cases, calculated results are compared with the measured as illustrated in Figure 14. It is shown that the maximum efficiency of the two systems appears close to the calculated results.

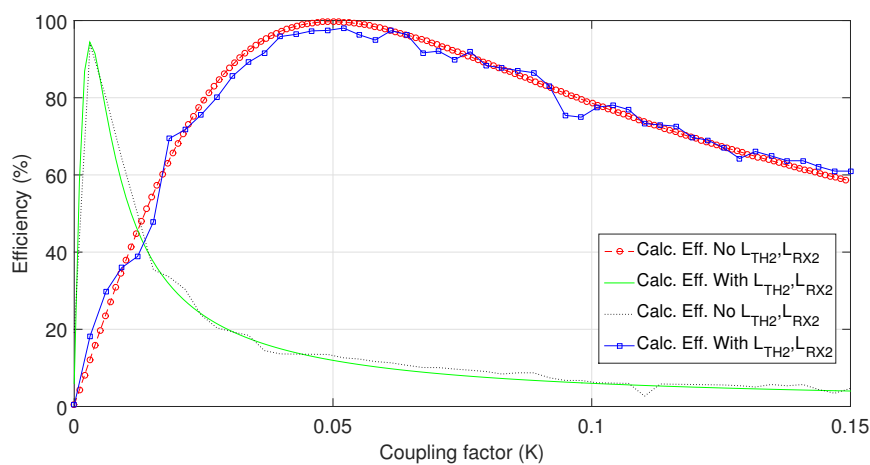


Figure 14. A comparison between the measured and calculated maximum distances between the low Q design coil with and without added inductor at frequency of 9.23 MHz. The system with an additional coil shows an increase in the distance between T_X and R_X at which maximum efficiency occurs.

Similar to the system with low quality of the coils, the new proposed system is compared with the conventional system with a high quality of the transmitter and receiver coils. Figure 15 shows a comparison between the two. As seen from the figure the system with high quality coils reaches its peak when the Q between the two coil reaches 0.004 and the maximum efficiency of the proposed design is reached when the coupling factor between the two coils is 0.003. As already mentioned, this occurs due to a desire to use widely available values of the capacitors. From the figure, we can see that the measured results from the prototype system closely follows the calculated results from the model. From the calculations, the maximum efficiency of the proposed system is 7% below that of the conventional model, however the advantages of the proposed design are shown in Table 4.

The main advantage of the proposed design is the reduced size of the loops. The length of the transmitter loop in the conventional design is equal to 15 mm while that of the proposed design is equal to 3 mm. Similar to the transmitter loop, the length of the receiver loop from the proposed design is 4 mm, which is a big improvement from the 20 mm required for the system from conventional design. Furthermore, the proposed system design has significantly reduced the weight of the WPT transmitter from 7.37 g in conventional system to 1.58 g while the receiver weight also improved from 8.63 g to 1.78 g. Both of the above advancements has lead to overall 80% reduction of its size and weight. Therefore, the size reduction offered by the proposed system is achieved at the cost of slight reducing the system efficiency.

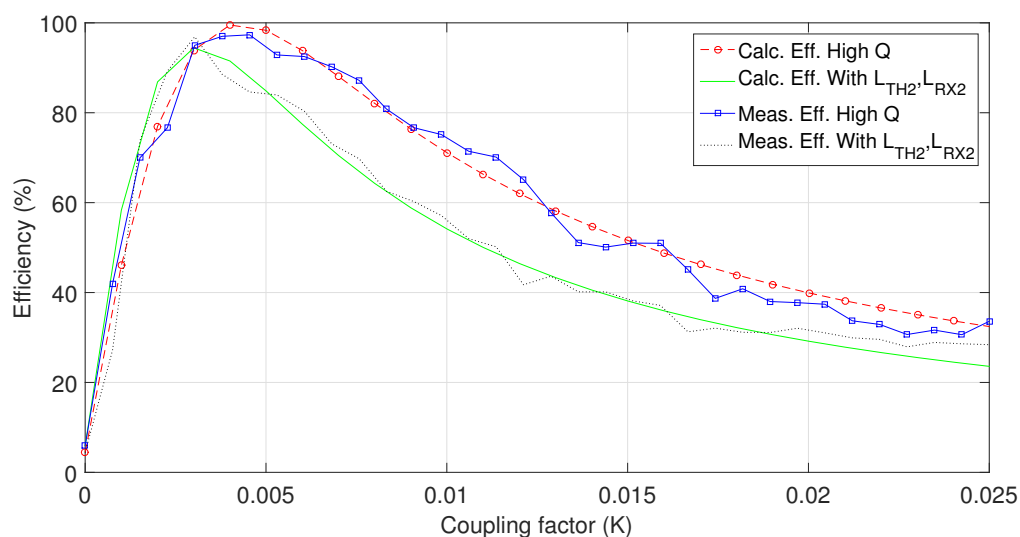


Figure 15. Comparison between measured and calculated maximum distances between the T_X and R_X coil between the system with high Q coils and the system with added inductor. The results show a similar distance of transmission that can be achieved with both systems.

Table 4. Comparison of the physical parameters of the conventional and modified systems. Proposed system shows a great improvement towards the conventional design.

	Conv. L_{TX}	Mod. L_{TX}	Diff. %	Conv. L_{RX}	Mod. L_{RX}	Diff. %
Length	15 mm	3 mm	80%	20 mm	4 mm	80%
Weight	7.37 g	1.58 g	78.6%	8.63 g	1.78 g	79.4%
Turns	41	8	80.5%	48	48	81%

6. Conclusions

A novel method of designing a two-loop strongly resonant WPT system is presented in this paper. In order to achieve a maximum distance, a high quality factor of the two coils must be achieved. However, this requires high inductance coils which eventually leads to an increased coil size as well

as the weight of the system and tends to use non-conventional size of the capacitors to specify the oscillating frequency. In this paper, a new concept of designing a two-loop strongly resonant WPT system is proposed. With this method the loops are designed in order to use a conventional high capacitors instead of usual low ones. As a consequence, smaller inductors are needed to specify the oscillating frequency and therefore the size of the inductors is reduced. To increase the quality factor, a new set of inductors are introduced to the design. A 5% decline in the WPT transfer efficiency is observed compared with the conventional method, however the size of the loop is reduced by 80% while the weight is reduced by 79%. Furthermore, simulation results are compared with measurements and they showed very similar trends.

Acknowledgments: This work is supported in part by “Smart In-Building Micro Grid for Energy Management” (EPSRC EP/M506758/1) through Innovate UK (Innovate UK Project 101836) and in part by the “Triangulum project” funded by the European Commission under the Horizon 2020 Smart Cities and Communities programme (Grant Agreement 646578-Triangulum-H2020-2014-20 151H2020-SCC-2014).

Author Contributions: Matjaz Rozman and Bamidele Adebisi conceived and designed the experiments; Matjaz Rozman performed the experiments; Matjaz Rozman, Tim Collins and Michael Fernando analyzed the data; Bamidele Adebisi and Khaled M.Rabie contributed reagents/materials/analysis tools; Matjaz Rozman and Khaled M.Rabie and Michael Fernando wrote the paper; Augustine Ikpehai and Rupak Kharel reviewed the manuscript.

Conflicts of Interest: The authors declare no conflict of interest.

References

1. Rabie, K.M.; Adebisi, B.; Rozman, M. Outage probability analysis of WPT systems with multiple-antenna access point. In Proceedings of the 2016 10th International Symposium on Communication Systems, Networks and Digital Signal Processing (CSNDSP), Prague, Czech Republic, 20–22 July 2016; pp. 1–5.
2. Rabie, K.M.; Adebisi, B.; Alouini, M.S. Wireless power transfer in cooperative DF relaying networks with log-normal fading. In Proceedings of the 2016 IEEE Global Communications Conference (GLOBECOM), Washington, DC, USA, 4–8 December 2016; pp. 1–6.
3. Lin, J.C. Wireless power transfer for mobile applications, and health effects [telecommunications health and safety]. *IEEE Antennas Propag. Mag.* **2013**, *55*, 250–253.
4. Dickinson, R.M. Power in the sky: Requirements for microwave wireless power beamers for powering high-altitude platforms. *IEEE Microw. Mag.* **2013**, *14*, 36–47.
5. Raible, D.E.; Dinca, D.; Nayfeh, T.H. Optical frequency optimization of a high intensity laser power beaming system utilizing VMJ photovoltaic cells. In Proceedings of the 2011 International Conference on Space Optical Systems and Applications (ICSOS), Santa Monica, CA, USA, 11–13 May 2011; pp. 232–238.
6. Lu, Y.; Ma, D.B. Wireless power transfer system architectures for portable or implantable applications. *Energies* **2016**, *9*, 1087.
7. Kim, S.; Ho, J.S.; Chen, L.Y.; Poon, A.S. Wireless power transfer to a cardiac implant. *Appl. Phys. Lett.* **2012**, *101*, 073701.
8. Kilinc, E.G.; Conus, G.; Weber, C.; Kawkabani, B.; Maloberti, F.; Dehollain, C. A system for wireless power transfer of micro-systems in-vivo implantable in freely moving animals. *IEEE Sens. J.* **2014**, *14*, 522–531.
9. Cook, N.P.; Sieber, L.; Widmer, H. Short Range Efficient Wireless Power Transfer. U.S. Patent 12,427,318, 21 April 2009.
10. Xie, L.; Shi, Y.; Hou, Y.T.; Lou, A. Wireless power transfer and applications to sensor networks. *IEEE Wirel. Commun.* **2013**, *20*, 140–145.
11. Jawad, A.M.; Nordin, R.; Gharghan, S.K.; Jawad, H.M.; Ismail, M. Opportunities and challenges for near-field wireless power transfer: A review. *Energies* **2017**, *10*, 1022.
12. Costanzo, A.; Dionigi, M.; Mastri, F.; Mongiardo, M.; Monti, G.; Russer, J.A.; Russer, P.; Tarricone, L. Conditions for a load-independent operating regime in resonant inductive WPT. *IEEE Trans. Microw. Theory Tech.* **2017**, *65*, 1066–1076.
13. Fotopoulou, K.; Flynn, B.W. Wireless power transfer in loosely coupled links: Coil misalignment model. *IEEE Trans. Magn.* **2011**, *47*, 416–430.

14. Li, Y.; Wang, Y.; Cheng, Y.; Li, X.; Xing, G. QiLoc: A Qi wireless charging based system for robust user-initiated indoor location services. In Proceedings of the 2015 12th Annual IEEE International Conference on Sensing, Communication, and Networking (SECON), Seattle, WA, USA, 22–25 June 2015; pp. 480–488.
15. Liu, X. Qi standard wireless power transfer technology development toward spatial freedom. *IEEE Circuits Syst. Mag.* **2015**, *15*, 32–39.
16. Van Wageningen, D.; Staring, T. The Qi wireless power standard. In Proceedings of the 14th International Power Electronics and Motion Control Conference EPE-PEMC 2010, Ohrid, Macedonia, 6–8 September 2010; pp. S15-25–S15-32.
17. Kim, J.; Son, H.C.; Kim, D.H.; Park, Y.J. Optimal design of a wireless power transfer system with multiple self-resonators for an LED TV. *IEEE Trans. Consum. Electron.* **2012**, *58*, doi:10.1109/TCE.2012.6311317.
18. Geng, Y.; Li, B.; Yang, Z.; Lin, F.; Sun, H. A high efficiency charging strategy for a supercapacitor using a wireless power transfer system based on inductor/capacitor/capacitor (LCC) compensation topology. *Energies* **2017**, *10*, 135.
19. Haldi, R.; Schenk, K.; Nam, I.; Santi, E. Finite-element-simulation-assisted optimized design of an asymmetrical high-power inductive coupler with a large air gap for EV charging. In Proceedings of the 2013 IEEE Energy Conversion Congress and Exposition, Denver, CO, USA, 15–19 September 2013; pp. 3635–3642.
20. Wen, F.; Huang, X. Optimal magnetic field shielding method by metallic sheets in wireless power transfer system. *Energies* **2016**, *9*, 733.
21. RamRakhyani, A.K.; Mirabbasi, S.; Chiao, M. Design and optimization of resonance-based efficient wireless power delivery systems for biomedical implants. *IEEE Trans. Biomed. Circuits Syst.* **2011**, *5*, 48–63.
22. Rozman, M.; Fernando, M.; Adebisi, B.; Rabie, K.M.; Kharel, R.; Ikpehai, A.; Gacanin, H. Combined conformal strongly-coupled magnetic resonance for efficient wireless power transfer. *Energies* **2017**, *10*, 498.
23. Kurs, A.; Karalis, A.; Moffatt, R.; Joannopoulos, J.D.; Fisher, P.; Soljačić, M. Wireless power transfer via strongly coupled magnetic resonances. *Science* **2007**, *317*, 83–86.
24. Somani, S.; Shaqfeh, E.S.; Prakash, J.R. Effect of solvent quality on the coil-stretch transition. *Macromolecules* **2010**, *43*, 10679–10691.
25. Junaid, A.B.; Konoiko, A.; Zweiri, Y.; Sahinkaya, M.N.; Seneviratne, L. Autonomous wireless self-charging for multi-rotor unmanned aerial vehicles. *Energies* **2017**, *10*, 803.
26. Dai, Z.; Wang, J.; Long, M.; Huang, H. A witrlicity-based high-power device for wireless charging of electric vehicles. *Energies* **2017**, *10*, 323.
27. Hwang, K.; Cho, J.; Kim, D.; Park, J.; Kwon, J.H.; Kwak, S.I.; Park, H.H.; Ahn, S. An autonomous coil alignment system for the dynamic wireless charging of electric vehicles to minimize lateral misalignment. *Energies* **2017**, *10*, 315.
28. Jiang, C.; Chau, K.T.; Liu, C.; Lee, C.H.T. An overview of resonant circuits for wireless power transfer. *Energies* **2017**, *10*, 894.
29. Liu, D.; Hu, H.; Georgakopoulos, S.V. Misalignment sensitivity of strongly coupled wireless power transfer systems. *IEEE Trans. Power Electron.* **2017**, *32*, 5509–5519.
30. Sample, A.P.; Meyer, D.T.; Smith, J.R. Analysis, experimental results, and range adaptation of magnetically coupled resonators for wireless power transfer. *IEEE Trans. Ind. Electron.* **2011**, *58*, 544–554.
31. Vijayakumaran Nair, V.; Choi, J.R. An efficiency enhancement technique for a wireless power transmission system based on a multiple coil switching technique. *Energies* **2016**, *9*, 156.
32. Kiani, M.; Jow, U.M.; Ghovanloo, M. Design and optimization of a 3-coil inductive link for efficient wireless power transmission. *IEEE Trans. Biomed. Circuits Syst.* **2011**, *5*, 579–591.
33. Jow, U.M.; Ghovanloo, M. Design and optimization of printed spiral coils for efficient transcutaneous inductive power transmission. *IEEE Trans. Biomed. Circuits Syst.* **2007**, *1*, 193–202.
34. Lee, H.; Kang, S.; Kim, Y.; Jung, C. Small-sized metallic and transparent film resonators for MR-WPT system. *Electron. Lett.* **2016**, *52*, 650–652.
35. Hu, H.; Liu, D.; Georgakopoulos, S.V. Miniaturized strongly coupled magnetic resonant systems for wireless power transfer. In Proceedings of the 2016 IEEE International Symposium on Antennas and Propagation (APSURSI), Fajardo, Puerto Rico, 26 June–1 July 2016; pp. 155–156.
36. Nguyen, V.T.; Kang, S.H.; Jung, C.W. Wireless power transfer for mobile devices with consideration of ground effect. In Proceedings of the 2015 IEEE Wireless Power Transfer Conference (WPTC), Boulder, CO, USA, 13–15 May 2015; pp. 1–4.

37. Fujita, T.; Yasuda, T.; Akagi, H. A wireless power transfer system with a double-current rectifier for EVs. In Proceedings of the 2016 IEEE Energy Conversion Congress and Exposition (ECCE), Milwaukee, WI, USA, 18–22 September 2016; pp. 1–7.
38. MahdaviFard, M.; Poorfakhraei, A.; Tahami, F. A novel method for reduction of coil weight and size in wireless power transfer. In Proceedings of the 2017 8th Power Electronics, Drive Systems Technologies Conference (PEDSTC), Mashhad, Iran, 14–16 February 2017; pp. 395–400.
39. Theilmann, P.T.; Asbeck, P.M. An analytical model for inductively coupled implantable biomedical devices with ferrite rods. *IEEE Trans. Biomed. Circuits Syst.* **2009**, *3*, 43–52.
40. Hu, H.; Georgakopoulos, S.V. Analysis and design of conformal SCMR WPT systems with multiple resonators. In Proceedings of the 2014 IEEE Antennas and Propagation Society International Symposium (APSURSI), Memphis, TN, USA, 6–11 July 2014; pp. 1347–1348.



© 2017 by the authors. Licensee MDPI, Basel, Switzerland. This article is an open access article distributed under the terms and conditions of the Creative Commons Attribution (CC BY) license (<http://creativecommons.org/licenses/by/4.0/>).